

Power Requirements for Superior H-mode Confinement on Alcator C-Mod: Experiments in Support of ITER

J.W. Hughes¹, A. Loarte², M.L. Reinke¹, J.L. Terry¹, D. Brunner¹, A.E. Hubbard¹,
B. LaBombard¹, B. Lipschultz¹, J. Payne¹, S. Wolfe¹, S.J. Wukitch¹

¹Massachusetts Institute of Technology, Plasma Science and Fusion Center, 175 Albany Street, Cambridge, Massachusetts 02139 USA

²ITER Organization, CS 90 046, 13067 Saint Paul lez Durance Cedex, France

E-mail: jwhughes@psfc.mit.edu

Abstract: Power requirements for maintaining suitably high confinement (*i.e.*, normalized energy confinement time $H_{98} \geq 1$) in H-mode and its relation to H-mode threshold power, P_{th} , are of critical importance to ITER. In order to better characterize these power requirements and to complement prior examinations on JET, recent experiments on the Alcator C-Mod tokamak have investigated H-mode properties, including the edge pedestal and global confinement, over a range of input powers near and above P_{th} . In addition, we have examined the compatibility of impurity seeding with high performance operation, and the influence of plasma radiation and its spatial distribution on performance. Experiments were performed at 5.4T at ITER relevant densities, utilizing bulk metal plasma facing surfaces and ion cyclotron range of frequencies waves for auxiliary heating. Input power was scanned both in stationary enhanced D_α (EDA) H-modes with no large ELMs and in ELMy H-modes in order to relate the resulting pedestal and confinement to the amount of power flowing into the scrape-off layer, P_{net} , and also to the divertor targets. In both EDA and ELMy H-mode, energy confinement is generally good, with H_{98} near unity. As P_{net} is reduced to levels approaching that in L-mode, pedestal temperature diminishes significantly and normalized confinement time drops. By seeding with low-Z impurities such as Ne and N_2 , high total radiated power fractions are possible ($P_{rad}/P_{in} \sim 0.7$), along with substantial reductions in divertor heat flux ($>4x$), all while maintaining $H_{98} \sim 1$. When the power radiated from the confined *vs.* unconfined plasma is examined, pedestal and confinement properties are clearly seen to be an increasing function of P_{net} , helping to unify the results with those from unseeded H-modes. This provides increased confidence that the power flow across the separatrix is the correct physics basis for ITER extrapolation. The experiments show that P_{net}/P_{th} of one or greater is likely to lead to $H_{98} \sim 1$ operation, and also that such a condition can be made compatible with a low-Z radiative impurity solution for reducing divertor heat loads to levels acceptable for ITER.

1. Introduction

Operation in high confinement mode, or H-mode, is a requirement for baseline operation in ITER and likely also for future toroidal fusion devices. It has been widely assumed that the fusion performance of ITER can be projected from an empirically determined energy confinement time, $\tau_{ITER-98(y,2)}$, which contains dependences on controllable engineering parameters such as magnetic field, plasma current and density [1]. However, when the measured H-mode confinement times, τ_E , of existing devices are normalized to $\tau_{ITER-98(y,2)}$, the resulting H-factor, known by the shorthand of H_{98} , tends to exhibit a considerable spread about unity. It is therefore important to understand whether there are key parameters that enhance or diminish τ_E and that are not captured in $\tau_{ITER-98(y,2)}$.

This paper describes research conducted on the Alcator C-Mod tokamak [2] with the goal of characterizing the role of both input and radiated power on normalized confinement, building on initial results discussed in [3]. We examine two key questions. First, what are the power requirements for maintaining suitably high confinement (*i.e.*, $H_{98} \geq 1$) in the resulting H-mode, and how do these requirements relate to the H-mode threshold power P_{th} ? Second, can the power requirements for superior H-mode performance be made compatible with an edge radiation solution for mitigating excess power loading on the tokamak divertor?

The first question is of critical importance to ITER, since present estimates [4] of P_{th} indicate it is only marginally lower than that available for heating H-mode plasmas in ITER. This is the case both for alpha-dominated plasmas during $Q_{DT}=10$ operation and for the earlier, non-activated phase, in which experimental strategies for controlling Type I edge localized modes (ELMs) must be developed. However, despite considerable efforts to characterize both H-mode confinement, and H-mode access conditions, this specific question has been studied in detail only on the JET tokamak [5]. In order to build on this work, recent experiments on C-Mod have investigated H-mode properties, including the edge pedestal, edge relaxation mechanisms and global confinement, at input power levels both close to and in excess of the H-mode threshold.

As will be shown below, the key parameter determining H-mode performance is the net power flowing through the plasma boundary, P_{net} . By seeding discharges with extrinsic impurities, we were able to establish this conclusively by regulating the amount of core radiated power, thus decoupling P_{net} from the total input power. This technique also enabled us to mitigate high divertor heat fluxes in H-mode with $H_{98}\sim 1$, in answer to the second question posed above. The ability to dissipate input power in this manner is also of critical importance for ITER [6], where the acceptable power loading on the divertor is estimated to be 15—30% of the total input power available. Reducing power to the divertor via edge radiation has been investigated on a number of devices in ELMy regimes (both Type I and Type III) in the past, but not necessarily while maintaining high confinement. [7,8,9,10,11]

2. Experimental Description

Alcator C-Mod typically operates at or near the ITER magnetic field and at ITER relevant densities, employs bulk metal plasma facing surfaces (Mo), and chiefly uses ion cyclotron range of frequencies (ICRF) waves for auxiliary heating. In the experiments described here, many of the Mo tiles were installed with a 0.1mm surface layer of boron, and overnight boronizations were performed prior to experimental run days in order to provide additional coatings for high-Z plasma facing components. [12] Two classes of ICRF-heated H-modes at $B_T=5.4T$ with $3.9 < q_{95} < 4.1$ were used in these experiments. The first consisted of stationary enhanced D_α (EDA) H-modes [13] with no large ELMs, with line-averaged density \bar{n}_e in the range of $2.5\text{--}3.0 \times 10^{20} \text{ m}^{-3}$. These were run in a conventionally shaped equilibrium for C-Mod, shown in Figure 1. The second class comprised ELMy H-modes with \bar{n}_e of $1.7\text{--}2.4 \times 10^{20} \text{ m}^{-3}$ and run using an atypical equilibrium with high lower triangularity (see Figure 1), which is known to promote access to ELMy H-mode [14]. Scans of loss power $P_{loss}=P_{oh}+P_{ICRF}-dW_{MHD}/dt$ and of $P_{net}=P_{loss}-P_{rad,core}$ were made in each case in order to correlate these with pedestal and confinement qualities. The ohmic power P_{oh} and the plasma stored energy W_{MHD} are taken from magnetic equilibrium reconstructions. The absorbed ICRF power P_{ICRF} is assumed to be 90% of the net launched ICRF power in all cases. Core radiation is characterized using a

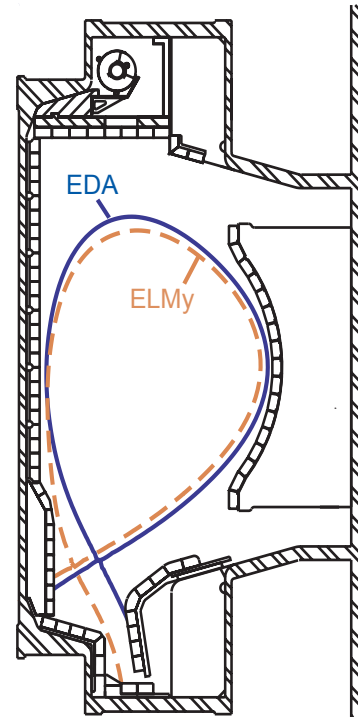


FIG 1: Examples of equilibria used to obtain EDA (blue solid) and ELMMy (orange dashed) H-modes

tangentially viewing array of resistive bolometers at the low-field side midplane [15]. The line-integrated brightness measurements are Abel inverted to obtain radial emissivity profiles, which are then integrated within the last closed flux surface (LCFS) to obtain the total core radiated power $P_{\text{rad,core}}$. Divertor heat flux is inferred using an infrared (IR) camera viewing a segment of the outer divertor and utilizing a 2D heat transport model for the divertor tiles to transform measured surface temperatures into heat flux profiles [16]. These profiles are then integrated over the divertor surface, assuming toroidal symmetry, to produce the total power conducted to the outer divertor $P_{\text{o-div}}$. Note that these heat flux measurements were not possible in the ELMy H-mode cases, since at present we are not set up to measure the profiles when the outer strike point is on the vessel “floor” (Figure 1).

The primary intrinsic impurities in C-Mod are molybdenum and boron, and these contribute to the radiated power in all H-modes. In a subset of EDA H-modes, power balance was regulated via extrinsic impurity seeding, in addition to varying input auxiliary heating. Gaseous impurities were injected from a fast piezoelectric valve positioned on the LFS of the main chamber, typically in advance and in some cases during the application of ICRF power. Argon, neon and nitrogen were evaluated separately as potential seed gases. A pleasing result is that with seeding, core intrinsic Mo concentration is mostly unaffected despite the increased potential for ion sputtering of plasma facing components. Effects of seeding on plasma performance and divertor heat loads will be discussed in Sections 4 and 5.

3. Unseeded H-modes

In both EDA and ELMy H-mode with only intrinsic impurity content (primarily Mo and B), energy confinement can be very good, with H_{98} generally near or above unity, provided sufficient heating power is available and core radiated power is sufficiently low, *i.e.* when $P_{\text{rad,core}}/P_{\text{loss}} < 0.4$. This is illustrated in Figure 2(a), where H_{98} is plotted versus the core radiated power fraction for EDA and ELMy H-mode, and also in L-mode cases close to the L-H transition. By carefully characterizing the net power through the boundary, as described above, we can identify a positive trend in H_{98} with respect to P_{net} . Figure 2(b) shows that this holds for both the EDA and ELMy data sets, with the EDA cases requiring somewhat higher net power to reach and exceed the $H_{98}=1$ condition.

As discussed above, the available power in H-mode on ITER will be marginal with respect to P_{th} projected using the empirical scaling law found in [4]. Therefore it is of interest to normalize experimental powers to this same scaling law, evaluated using concurrent C-Mod discharge parameters (*i.e.* density, toroidal field, plasma surface area) as inputs. Figures 2(c—d) show that $H_{98} > 1$ is favored by either $P_{\text{loss}}/P_{\text{th}} > 1.5$ or $P_{\text{net}}/P_{\text{th}} > 1.0$. They also show that H_{98} in each H-mode regime (EDA or ELMy) is better correlated with P_{net} than with P_{loss} , indicating that power flow into the scrape-off layer (SOL) is the correct physical metric for setting global confinement. This confirms the current assumption being used for ITER.

Comparison of Figures 2(b,d) shows that dividing P_{net} by P_{th} provides a useful organization of the EDA and ELMy data, such that the normalized confinement scales with normalized net power in the same way between the two H-mode regimes. This does not imply that the L-H threshold physics is important in determining the H-mode confinement; it is likely that the normalization is effectively accounting for the systematic difference in plasma density observed between EDA and ELMy H-modes at otherwise similar plasma parameters. Figure 2(e) demonstrates that edge density in ELMy H-mode is reduced by a factor of $\sim 2x$ relative to EDA, and so it is perhaps unsurprising that higher edge temperature and overall confinement is achievable with lower absolute power. Confinement enhancement (or

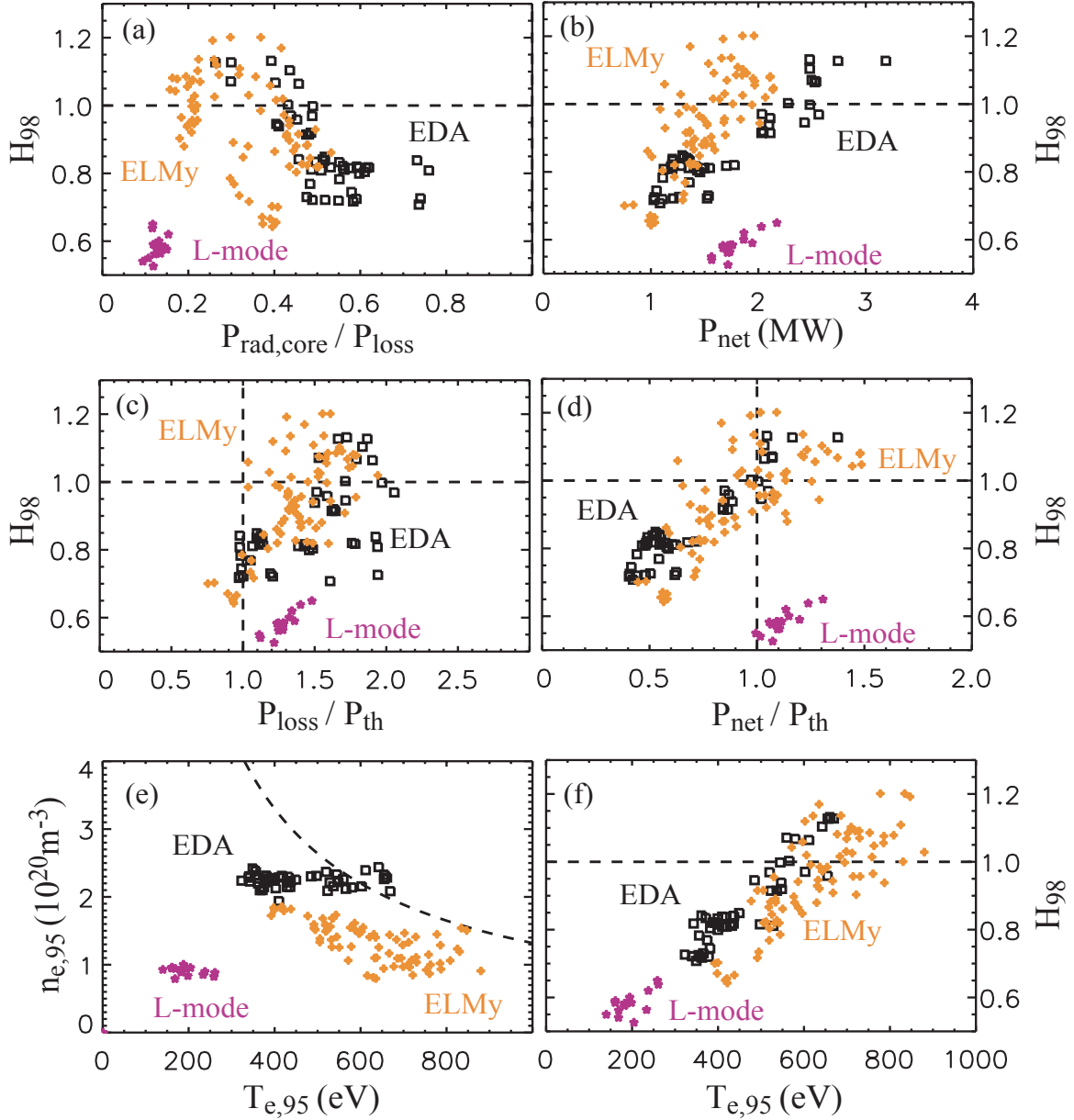


FIG 2: Confinement in L-mode and EDA, ELMy H-modes with intrinsic impurity content only, as a function of (a) $P_{rad,core}/P_{loss}$ (b) P_{net} (c) P_{loss}/P_{th} (d) P_{net}/P_{th} and (f) pedestal T_e . Pedestal n_e and T_e are shown in (e) along with a dashed curve representing a constant electron pressure.

degradation) in these H-modes appears to be correlated entirely with the regulation of the edge pedestal through edge power flux, with stiff core thermal transport providing the additional leverage on global confinement [17]. The strong correlation of edge T_e and H_{98} is shown in Figure 2(f). Note that, for a given temperature, the high density EDA H-modes have better performance than the low density ELMy H-modes.

For completeness, the actual value of H-mode threshold power was characterized in the EDA equilibrium on the actual experimental run days, for comparison with the scaling law. This was done using slow ramps and staircase waveforms for auxiliary power, then noting the P_{loss} value at the transition time. This measurement gave 1.75 ± 0.35 MW for nominally identical target plasmas, with the most significant variation observed between different experimental days. As is common with H-mode studies, hidden variables seem to play a significant role in setting the power threshold. The low end of this range is close to the scaling law P_{th} , as can be

gleaned from the L-mode data included in Figure 2(c). Also noteworthy in these results, and evinced in Figures 2(b—d) is the significant power hysteresis [18] evident in the L-H-L cycle. H-mode can be sustained, though not necessarily with high H_{98} , with significantly less power than is needed to trigger its formation. As P_{net} is reduced to levels approaching that in L-mode, pedestal temperature diminishes significantly and normalized confinement time drops. These changes appear to happen continuously, and, while Type III ELMs and dithering can be observed in the most weakly powered H-modes, this is observed in a relatively narrow window in $P_{\text{loss}}/P_{\text{th}}$, in both EDA and ELMy H-mode configurations.

4. EDA H-modes with Impurity Seeding

As noted above, an additional knob on the net power is the capability to seed with controlled amounts of extrinsic impurity. EDA discharges seeded with varying amounts of Ar, Ne and N_2 confirm that P_{net} plays a dominant role in determining H_{98} , at least when $P_{\text{net}}/P_{\text{th}}$ is close to unity. Shown in Figure 3 are data from seeded EDA H-modes along with the unseeded EDA data set from Figure 2. As explained in Reference 3, a subset of these discharges, mainly consisting of Ne-seeded cases, was found to have unusually high wall neutral pressure and SOL neutral density, and this was found to correlate with a reduction in confinement even at high $P_{\text{net}}/P_{\text{th}}$. Subsequently it was found that by ignoring data points with n_e at the LCFS greater than $1.7 \times 10^{20} \text{ m}^{-3}$, the outlying data were also mostly eliminated. This criterion has been applied to the seeded data analyzed herein. Examples of the excluded data are shown in Figure 3(b) as gray symbols.

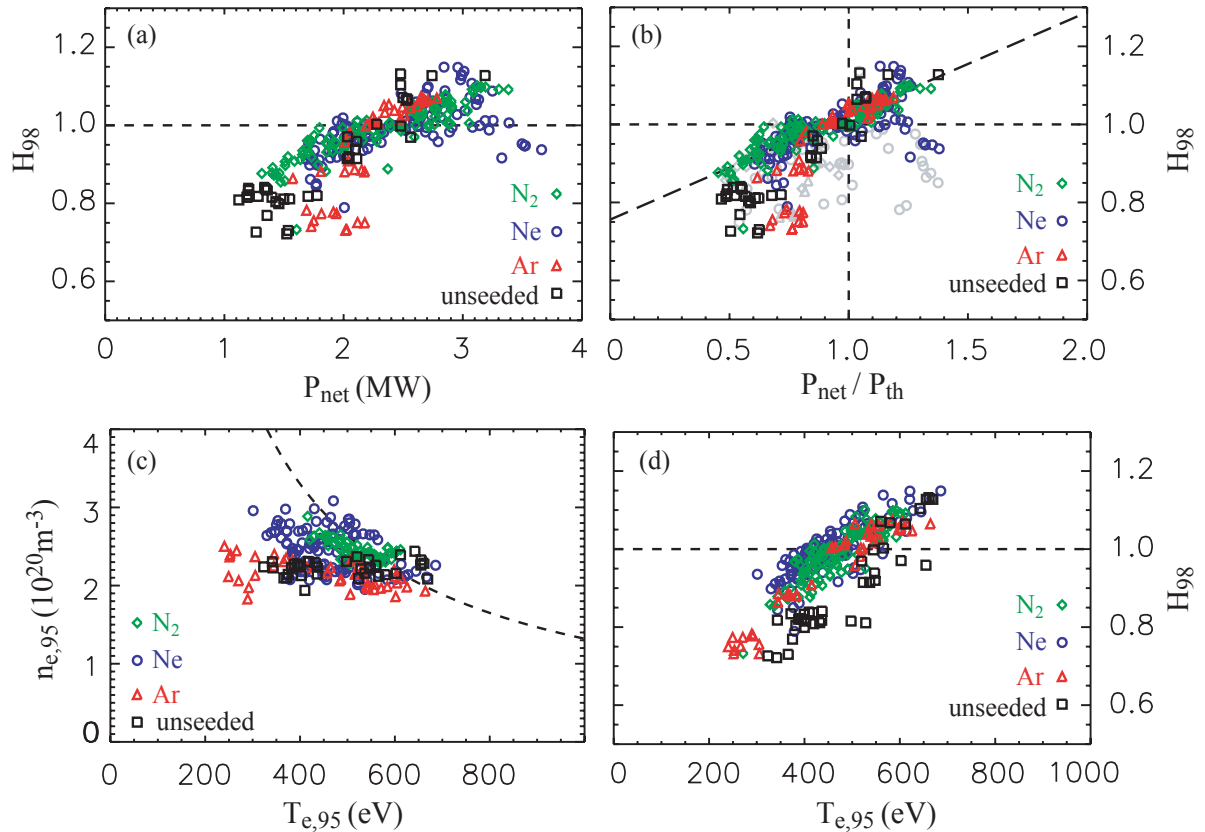


FIG 3. Confinement in EDA H-modes with intrinsic impurity content only (black) and seeded with Ar, Ne and N_2 , as a function of (a) P_{net} , (b) $P_{\text{net}}/P_{\text{th}}$ and (d) pedestal T_e . Pedestal n_e and T_e are shown in (c) along with a dashed curve representing a constant electron pressure. All cases shown have $n_{e,\text{LCFS}} < 1.7 \times 10^{20} \text{ m}^{-3}$, with the exception of the grayed symbols in (b).

Much as in the comparison between EDA and ELMy H-mode in Section 3, H_{98} correlates well with $P_{\text{net}}/P_{\text{th}}$. The dependence of H_{98} on net power is nearly identical among all discharges with $P_{\text{net}}/P_{\text{th}}$ between about 0.8 and 1.3, and can be approximated with a linear function [dashed line in Figure 3(b)]. For low Z seed species (Ne, N_2) the linear trend extends to lower values of normalized power, while underpowered Ar-seeded and unseeded H-modes show a more dramatic decrease in H_{98} . At higher power ratios, it is not clear whether H_{98} saturates, and at what value of $P_{\text{net}}/P_{\text{th}}$ this might happen. Extending this power ratio to values of 1.5 or greater in seeded discharges is challenging because the core radiation must be balanced by increasingly large values of auxiliary input power (*i.e.* $>5\text{MW}$).

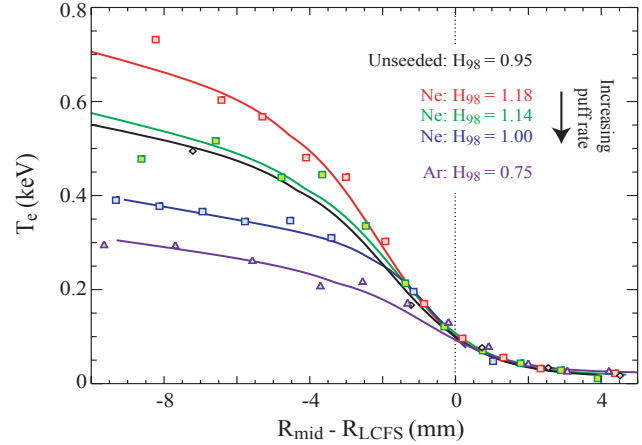


FIG 4. Examples of temperature pedestals without seeding and with impurity seeding from Ne and Ar.

For reasons that are unclear, the low- Z impurity seeding allows the H-mode to support a higher pedestal n_e (and thus p_e) for a given T_e . This is shown in Figure 3(c), which combines the pedestal parameters in seeded H-modes with the unseeded EDA cases from Figure 2(e). This may be a factor in sustaining $H_{98} \geq 0.9$ with low Z seeding even at $T_{e,95} < 400$ eV, an effect clearly seen in Figure 3(d). The edge pedestal was well-resolved with Thomson scattering in many of these discharges, allowing for improvement upon earlier studies of the pedestal with impurity seeding. [19] Examples of edge T_e profiles are compared in Figure 4. A wide variation in core radiated power is present in the five cases shown. The case with the lowest $P_{\text{rad,core}}$ is Ne seeded with $H_{98} \sim 1.2$ and a pedestal height of greater than 500 eV. Increasing the puff rate of Ne increases $P_{\text{rad,core}}$ and decreases the T_e pedestal, ultimately to well below the 400 eV characteristic of an unseeded EDA H-mode with $H_{98} \sim 1$. A heavily seeded Ar case is also shown, with pedestal and confinement substantially reduced, and very near the H-L transition point. Though average temperature gradients in the pedestal do increase as the pedestal height rises, we also find that the width of the temperature pedestal, as derived from a modified tanh fit [20], also appears to increase slightly with temperature when $T_{e,\text{PED}} > 400$ eV. Prior pedestal scaling studies [20] in unseeded EDA H-mode collected very few data at such high values of $T_{e,\text{PED}}$, and so could not have resolved such width variation.

5. Reduction in Power to the Divertor

When seeding EDA H-mode plasmas with low- Z impurities, a substantial reduction in divertor heat flux can be obtained without a significant degradation in energy confinement. As shown in Figure 5(a), the inferred power deposited on the outer divertor, obtained from IR measurements as described in Section 2, shows very dramatic reductions as the seed impurity Z decreases. In particular, $H_{98} \sim 1$ operation with N_2 seeding results in an outer divertor power load (0.2—0.3MW) that is reduced by a factor of about four from that in unseeded operation with similar confinement. (IR data are unavailable for the N_2 -seeded discharges with H_{98} significantly above 1.0.) In these best cases, the power falling on the outer divertor represents a remarkably small 5% of P_{loss} [See Figure 5(b)]. Solutions for ITER require that this fraction be between 10 and 20%.

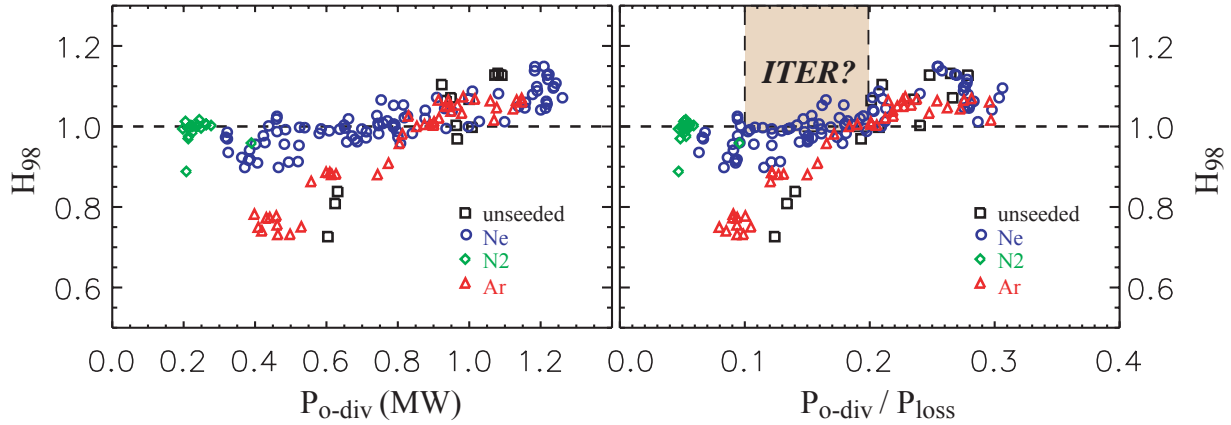


FIG 5: Low-Z impurity seeding of EDA H-modes demonstrates the capability to reduce power to the outer divertor by a substantial factor, while maintaining $H_{98} \sim 1$. (a) H_{98} vs. power to the outer divertor. (b) H_{98} vs. the fraction of loss power (approx. equal to input power) falling on the outer divertor. A critical question is whether ITER can operate within the pink box.

This effect is most readily achieved with 4–5 MW of ICRF heating, and $P_{\text{rad,core}} \sim 2$ MW, which provides ample P_{net} for the $H_{98} \geq 1$ regime. With Ne or N_2 as the seed impurity, one expects the radiated power distribution to shift more strongly toward the edge regions, including the divertor and SOL, allowing the main chamber radiated power P_{rad} to exceed the $P_{\text{rad,core}}$ by a substantial margin in these cases. Indeed, a wide angle bolometer, which views the core plasma as well as a portion of the divertor area, measures a P_{rad} approaching 70% of the input power in low-Z seeded discharges with $H_{98} \sim 1$. This “total” radiated power fraction is roughly double that observed in an unseeded EDA H-mode of similar confinement quality. By contrast, when Ar is used to increase P_{rad} to the same level, $P_{\text{rad,core}}$ is much higher, and confinement degrades to $H_{98} \sim 0.75$. Directly measured radiation profiles show variation with impurity species in P_{rad} contributions from the core and edge regions. Approximately 25% more power is lost inside the LCFS for Ar seeded plasmas compared to Ne and N_2 , leading to increased ratios of $P_{\text{net}}/P_{\text{loss}}$ [3].

6. Discussion and Future Work

This research addresses important considerations for ITER, and other future burning plasma devices. First, these experiments provide increased confidence that the power flow across the separatrix P_{net} is the correct physics basis for projecting the pedestal and confinement. Specifically, core radiated power must not be ignored in determining corrections to H_{98} based on power, while the amount of SOL/divertor radiation appears less important. This is seen to be true in both EDA and ELMy H-mode, and also independent of whether discharges are seeded with extrinsic impurities. Normalizing P_{net} to the L-H threshold power is a useful way of organizing the data and gives a metric which might be easily considered for ITER. If H-mode confinement in ITER trends similarly to that in these C-Mod experiments, then $P_{\text{net}} \sim P_{\text{th}}$ will be sufficient to obtain $H_{98} \sim 1$ as desired. This condition is likely achievable on ITER.

It is by no means clear that normalizing net power to the L-H threshold scaling law is the correct approach, beyond the convenient fact that P_{th} has a near-linear density dependence that is required to organize the data set. Alternate normalizations may exist which better capture the relevant physics of the established H-mode edge transport barrier. Since this experiment produced a large number of underpowered H-modes with back-transitions to L-mode, there is potential in the future to use this data set to explore normalizing power with the measured

H-L back-transition threshold. Actually developing a scaling law for this power threshold would require a substantially greater effort, folding in the results from multiple devices.

The second major result of this research is the demonstration that substantial fractions of input power can be radiated effectively using low-Z impurity seeding while still meeting or exceeding the ITER scaling law for energy confinement time. In fact, many of the H-modes with highest performance on C-Mod (H_{98} up to ~ 1.2) are those that take advantage of impurity seeding. Seeding is found to be highly compatible with the use of ICRF auxiliary heating with metallic plasma facing components, as will be needed on ITER. In fact, for reasons that are not well understood at present, ICRF performance tends to be enhanced with seeding, as epitomized by reduced numbers of metallic injections and fewer transmitter faults. [12] Increasingly, operation with Ne or N_2 seeding is being considered for high-performance H-mode experiments. It should however be noted that even with seeding first-wall boronization remains a requirement for good H-mode performance.

Finally, we have demonstrated that it is possible to reduce divertor power loads to levels that meet and even undercut ITER operational requirements, all while maintaining sufficient P_{net} for $H_{98} \geq 1$. This result is potentially a major step forward in developing a radiative divertor solution of ITER H-mode. It should be remembered however, that this has to date been accomplished in a very small range of parameter space on C-Mod, and in a class of H-mode (EDA) which due to its high collisionality is not expected to be observed on ITER. Future work is aimed at expanding the operational space over which these good confinement and benign edge radiation conditions are simultaneously achieved.

This work was supported by US. Dept. of Energy Agreement DE-FC02-99ER54512.

-
- [1] DOYLE, E.J. *et al.* Nucl. Fusion **47** (2007) S18.
 - [2] MARMAR, E.S. AND ALCATOR C-MOD GROUP, Fusion Sci. Technol. **51** (2006) 261.
 - [3] REINKE, M.L. *et al.* "Effect of N_2 , Ne and Ar seeding on Alcator C-Mod H-mode confinement" accepted for publication in J. Nucl. Mater.
 - [4] MARTIN, Y.R. *et al.* Journal of Physics: Conference Series **123** (2008) 012033.
 - [5] SARTORI, R. *et al.* Plasma Phys. Control. Fusion **46** (2004) 723.
 - [6] LOARTE, A. *et al.* Nucl. Fusion **47** (2007) S203.
 - [7] GOETZ, J.A. *et al.* Phys. of Plasmas. **6** (1999) 1899.
 - [8] MONIER-GARBET, P. *et al.* Nucl. Fusion. **45** (2005) 1404.
 - [9] PETRIE, T.W. *et al.* J. Nucl. Mater. **363-365** (2007) 416.
 - [10] ASAKURA, N. *et al.* Nucl. Fusion. **49** (2009) 115010.
 - [11] GRUBER, O. *et al.* Nucl. Fusion. **49** (2009) 115014.
 - [12] WUKITCH, S.J. *et al.* "ICRF Impurity Behavior with Boron Coated Molybdenum Tiles in Alcator C-Mod", this conference EXD/P3-37.
 - [13] GREENWALD, M. *et al.* Fusion Sci. Technol. **51** (2007) 266.
 - [14] TERRY, J.L. *et al.* J. Nucl. Mater. **363-365** (2007) 994.
 - [15] REINKE, M.L. *et al.* Rev. Sci. Instrum. **79** (2008) 10F306.
 - [16] TERRY, J.L. *et al.* "Measurements of heat-flux profiles on the divertor target of Alcator-C-Mod using IR thermography", accepted for publication in Rev. Sci. Instrum. (2010).
 - [17] GREENWALD, M. *et al.* Nucl. Fusion **37** (1997) 793.
 - [18] HUBBARD, A.E. *et al.* Plasma Phys. Control. Fusion **44** (2002) A359.
 - [19] HUBBARD, A.E. *et al.* "Pedestals and confinement in Alcator C-Mod H-modes" 26th EPS Conference on Controlled Fusion and Plasma Physics, Maastricht (1999), Europhysics Conference Abstracts **23J** 13—16.
 - [20] HUGHES, J.W. *et al.* Phys. Plasmas **9** (2002) 3019.